

No-reference Blur Assessment Based on Edge Modeling

Jingwei Guan^a, Wei Zhang^{a,*}, Jason Gu^b, Hongliang Ren^c

^aSchool of Control Science and Engineering, Shandong University, Jinan, China

^bDepartment of Electrical and Computer Engineering, Dalhousie University, Halifax, NS, Canada

^cDepartment of Bioengineering, National University of Singapore, Singapore

Abstract

This paper presents a no-reference objective blur metric based on edge model (EMBM) to address the image blur assessment problem. A parametric edge model is incorporated to describe and detect edges, which can offer simultaneous width and contrast estimation for each edge pixel. With the pixel-adaptive width and contrast estimations, the probability of detecting blur at edge pixels can be determined. Also, unlike previous work, we advocate using only the salient edge pixels to simulate the blur assessment in Human Visual System (HVS). Finally, the blur metric is obtained by cumulating the probability of blur detection. Various images with different blur distortions are tested to demonstrate the effectiveness of the proposed metric.

© 2011 Published by Elsevier Ltd.

Keywords: Image quality assessment, No-reference, HVS, Perception, Blur metric, Edge model.

1. Introduction

Benefiting from the widespread use of imaging devices such as digital cameras and smartphones, millions of photographs are taken every day. Especially, the emergence of Internet has enabled sharing of photographs on a truly massive scale. Distinguishing the high perceptual quality images from the distorted poor ones in a subjective way is burdensome for human, and infeasible in real-time applications. Hence, developing objective assessment metrics to automatically find the high quality images is getting more and more attention as they are crucial for many fields such as image processing and multimedia.

A number of objective quality assessment metrics have been proposed, which can be classified into full-reference, reduced-reference and no-reference metrics based on the availability of the original image [1]. A full-reference quality assessment metric requires the whole original information of the reference image to give a quality score [2, 3, 4, 5]. The reduced-reference metrics only need part of the original information [6, 7, 8, 9, 10, 11, 12, 13, 14], and the no-reference metrics are the solutions in situations where the reference images are unavailable. Apparently, the no-reference metrics are more promising in applications and also more challenging.

In this work, we only focus on the image blurring problem which is one of the most common distortions and results in the loss of details in images. Blurring is mostly caused by the unideal imaging situation during acquisition process or the inappropriate filtering/compression during postprocessing process. Recently, there exist some no-reference objective assessment algorithms [15, 16, 17, 18, 19, 20, 21, 22, 23, 24, 25, 26, 27, 28] that attempted to interpret

*Corresponding author.

Email address: davidzhangsdu@gmail.com (Wei Zhang)

the perceptual quality in terms of image blurriness. Hassen et al. [15, 16] proposed a metric to achieve image blur assessment on the basis of Local Phase Coherence (LPC) in the wavelet domain. Since edges in an image vary in LPC, a sharpness index can be obtained by quantifying the degree of LPC for each edge pixel. Vu et al. [17] also proposed a wavelet based sharpness metric by decomposing the image via discrete wavelet transform (DWT). The image sharpness is measured via a weighted average of the log-energies of the DWT subbands. Blanchet et al. [18] defined a metric named Global Phase Coherence (GPC) based on the regularity of random phase images. Such metric was improved in [19] by using Gaussian random field to reduce the computational complexity. In [20], Marziliano et al. presented a blur metric to measure the spread of the edges based on the smoothing or smearing effect of filtering or compression in JPEG2000 images. The edge width is calculated by counting the number of pixels with increasing grayscale values from one side and the number of pixels with decreasing grayscale values from the other side. Tang et al. [21] proposed a metric based on the low-level features to predict the quality of blur images. The low-level features are derived from a learning framework to correlate with the perceptual image quality. Mittal et al. [22] built the quality-aware visual words by clustering features such as SIFT computed from multiple patches across all collected images based on natural scene statistics (NSS). Then, the image quality was determined by examining the distributions of visual words.

To simulate well with the Human Visual System (HVS), some no-reference objective image blur metrics [23, 24] were proposed based on the concept of Just Noticeable Blur (JNB). The pioneering work was done in Just Noticeable Blur Metric (JNBM) [23] which indicated that HVS is able to mask blurriness around an edge up to a certain threshold. This threshold corresponds to the maximum amount of blurriness without being perceived by human eyes at a specific contrast, and thus is referred as “Just Noticeable Blur”. Through a lot of subjective experiments, the authors found the JNBs under different contrasts and derived a metric based on the probability summation model. Since JNBM missed the fact that the blur below JNB is unlikely to be perceived, Narvekar and Karam [24] presented an improved blur metric named Cumulative Probability of Blur Detection (CPBD) by introducing the concept of JNB into a cumulative probability model.

As the most important cues of images, edges are vital to the performance of image blur assessment. In this paper, we propose an improved objective metric by integrating the concept of edge modeling into JNB. To overcome the limitation of edge detection in JNBM and CPBD, a parametric edge model is incorporated for edge description and detection. Benefiting from this model, all edges in an image are depicted parametrically. The width and contrast for each edge pixel (see Sec.2.2 for details) can be computed simultaneously. Compared to the integer pixel-level width defined in CPBD and JNBM, the width here originates from the standard deviation of the blurring distortion and is more accurately floating-point. Moreover, edge model offers contrast estimation for each edge pixel. Thus our algorithm is simpler and does not need to perform block by block. More importantly, JNB is assigned to each pixel adaptively according to its contrast. Finally, with the aid of edge model, all edges can be detected well including the horizontal ones missed in CPBD and JNBM. Unlike previous work, we advocate using only the salient edge pixels that refer to the ones with large contrast for quality assessment. Because the salient edges are normally located at the boundary area containing two adjacent parts with distinct color and thus grab most attention from human visual perception.

2. The Algorithm

2.1. JNB-based Metrics

The aim of this paper is to overcome the limitation of conventional JNB-based image blur metrics like JNBM and CPBD by modeling edges in a parametrical way. So we shall first give a brief review about how they perform image blur assessment. JNBM and CPBD are very similar in the workflow where the image is first divided into blocks with the size of 64×64 . Then the divided blocks are classified into edge blocks and smooth blocks based on the percentage of edge pixels. The smooth ones are skipped in the quality assessment. Dividing an image into blocks can help determine the contrast, and the contrast of each block is fixed by subtracting the maximum value to the minimum value. According to the subjective test in [23], the JNB of each edge in a block are measured to be 5 for block contrast that is below or equal to 50 and 3 for block contrast is above 50.

Similar to [20], the width of each edge pixel is obtained in pixel level by counting the number of pixels with increasing grayscale values from one side and the number of pixels with decreasing grayscale values from the other side. With edge width, the probability of detecting a blur distortion for each edge pixel can be calculated as:

$$P_{BLUR}(e_i) = 1 - \exp(-|\frac{w(e_i)}{w_{JNB}(e_i)}|^\beta), \quad (1)$$

where $w(e_i)$ denotes the edge width detected around the i^{th} edge pixel e_i . $w_{JNB}(e_i)$ denotes the JNB width corresponding to the maximum amount of blurriness around the edge pixel e_i without being perceived by human at its contrast. The value of β is obtained by means of least squares fitting and normally set to 3.6. Apparently, P_{BLUR} increases as the edge blurriness increases. When $w_{JNB}(e_i) = w(e_i)$, the corresponding probability of detecting blur is 63%, i.e., $P_{JNB} = 63\%$. However, JNBM misses the fact that the blur is unlikely to be perceived when it is below JNB. Therefore, based on the assumption that the blur below JNB cannot be detected, CPBD is presented in [24] to only correspond to the percentage of edges where blur cannot be detected. As shown in (2), the metric is calculated by cumulating the probability of blur detection P_{BLUR} below P_{JNB} , and a higher value indicates a sharper image.

$$\text{Metric} = P(P_{BLUR} \leq P_{JNB}) = \sum_{P_{BLUR}=0}^{P_{BLUR}=P_{JNB}} P(P_{BLUR}). \quad (2)$$

However, CPBD and JNBM share some common limitations on edge computation. First, the edge width can only achieve pixel-level accuracy and is obtained by counting the numbers of pixels with increasing and decreasing grayscale around an edge pixel. Second, the quality assessment has to be performed block by block, and thus contrast is fixed for all edge pixels within one block. Not only is it inconvenient for the metric to operate, but the fixed block-based contrast is inappropriate for the quality assessment of each pixel. Because each block consists of edge pixels with different blurriness, and a contrast adaptive to each edge pixel is more promising to measure the unique blur distortion. Moreover, since contrast is fixed for all pixels within one block, CPBD and JNBM cannot pick out the salient edges that grab most attention from human perception for blur assessment. Also, removing the smooth blocks from metric computation by hardly thresholding the number of the edge pixels is thoughtless. Finally, it is found that they failed to detect the horizontal edges as illustrated in Fig. 1.

2.2. Edge Model

To well utilize the edge information for blur assessment, a parametric edge model [30, 31] is incorporated for edge description and detection in this work. Since edges in 2-D images can be characterized by sharp intensity changes in one direction, 1-D notation is used to explain the edge model as follows. A step edge at x_0 can be represented by $e(x; b, c, x_0) = cU(x - x_0) + b$ where $U(\bullet)$ is the unit step function. b denotes the edge basis. c represents the edge contrast. As shown in Fig. 2(a), a typical edge $s(x; b, c, w, x_0)$ can be regarded as a smoothed step edge which is obtained by convolving $e(x; b, c, w, x_0)$ with a 1-D Gaussian filter $g(x; w) = \frac{1}{\sqrt{2\pi w^2}} \exp\left(\frac{-x^2}{2w^2}\right)$ and so

$$s(x; b, c, w, x_0) = b + \frac{c}{2} \left(1 + \operatorname{erf}\left(\frac{x - x_0}{w\sqrt{2}}\right)\right), \quad (3)$$

where $\operatorname{erf}(\bullet)$ is the error function. w originates from the standard deviation of the blurring kernel and can be referred as the edge width parameter. With this model, the width and contrast estimation of an edge can be conducted pixel by pixel along the edge. That is, each pixel on the edge will have a unique width estimate and contrast estimate. Hence, we define $w(e_i)$ and $c(e_i)$ to represent the edge width and contrast detected around the i^{th} edge pixel e_i respectively. As shown in Fig. 2(b), the edge is sharper when w becomes smaller. All edges can be depicted parametrically by fitting (3) on them. Such fitting process includes two parts: edge detection and parameter estimation.

Similar to that of Canny, edge detection is done by convolving $s(x; b, c, w, x_0)$ with the derivative of a predefined Gaussian filter $g'_d(x; \sigma_d)$. The response is:

$$d(x; c, w, \sigma_d, x_0) = s(x; b, c, w, x_0) * g'_d(x; \sigma_d) = c \cdot g(x - x_0; \sqrt{w^2 + \sigma_d^2}) = \frac{c}{\sqrt{2\pi(w^2 + \sigma_d^2)}} \exp\left(\frac{-(x - x_0)^2}{2(w^2 + \sigma_d^2)}\right). \quad (4)$$

By sampling (4) at $x = 0, a, -a$, three measurements $d_1 = d(0; c, w, \sigma_d, x_0)$, $d_2 = d(a; c, w, \sigma_d, x_0)$ and $d_3 = d(-a; c, w, \sigma_d, x_0)$ near the peak can be obtained. The width and contrast for each edge pixel can be estimated as follows:

$$w = \sqrt{a^2/\ln(l_1) - \sigma_d^2} \quad (5)$$

$$c = d_1 \cdot \sqrt{2\pi a^2/\ln(l_1)} \cdot l_2^{1/a} \quad (6)$$

where $l_1 = \frac{d_1^2}{d_2 d_3}$, $l_2 = \frac{d_2}{d_3}$. The value of a can be chosen freely and normally $a = 1$.

2.3. Edge Model based Blur Metric (EMBM)

A block diagram showing the process of the proposed metric is given in Fig. 3. Given an image, we first detect the edges and estimate the width and contrast for each edge pixel based on edge model. As aforementioned, salient edges receive most attention from human perception because they are always located at the boundary area containing two adjacent parts with distinct color. With the pixel-adaptive contrast $c(e_i)$, salient edges can be picked out by thresholding for the following metric computation. Unlike JNBM and CPBD, since the edge width defined herein originates from the standard deviation of the blurring distortion, the JNB value also refers to the standard deviations of blurring. Based on the JNB table in [23], the pixel-adaptive JNB width $w_{JNB}(e_i)$ can be obtained based on $c(e_i)$ using (7). Finally, the probability of detecting blur of each edge pixel P_{BLUR} can be determined using (1). Similar to CPBD, the metric only corresponds to the percentage of edges where blur cannot be detected. As shown in (2), the metric is calculated by only cumulating the probability of blur detection below $P_{JNB}(e_i)$.

$$w_{JNB}(e_i) = \begin{cases} 0.8, & \text{if } c(e_i) \leq 50 \\ 0.72, & \text{if } c(e_i) \geq 51 \end{cases} \quad (7)$$

Specifically, we advocate using only the salient edge pixels referred as the ones with large contrast for blur assessment as shown in Fig. 4. Because salient edges locate at the boundary area containing two adjacent parts with distinct color and thus grab most attention from human visual perception. The other edges (non-salient edges) have weak contrasts and are sensitive to noise. The incorporation of edge modeling makes it easy to select the salient edges by thresholding with c_T . We found that $c_T = 8$ works well for all tests. If the contrast of an edge pixel is below c_T , it is regarded as unstable weak edge and excluded from the blur assessment. Otherwise, this edge is referred as the salient ones and its width will contribute to the metric computation.

With the aid of edge model, all edges can be detected well including the horizontal ones missed in CPBD and JNBM as shown in Fig. 1. Moreover, edge model offers simultaneous estimation of width and contrast for all edge pixels. As stated in Sec. 2.2, the edge width defined in edge model originates from the standard deviation of the blurring distortion and can achieve floating-point precision, while JNBM and CPBD focus on the variance in grayscale which can only get pixel-level width. Also compared to CPBD and JNBM, our algorithm is simpler and does not need to perform block by block as shown in Fig. 3.

3. Experimental Results

3.1. Test on Edge Width Estimation

Since edge width estimation is the basis for image blurriness assessment, comparative experiments are conducted to test the accuracy of edge width estimation of the proposed metric.

Fig. 5(a) shows an image with concentric rings. The circle shape is chosen to test edge detection performance in all directions. Also, to indicate the influence of adjacent edges in edge estimation, the concentric rings are designed to have different diameters and the distance between them varies as well. Next, we generate the blurry images using Gaussian filter with different standard deviations (σ) and additive Gaussian noise. Fig. 5(b) shows a blurred example when $\sigma = 2$. Then, edge detection and width estimation are performed on these blurry images. Fig. 5(c) shows the edge detection result produced by CPBD and JNBM. Similar to Fig. 1, the horizontal or semi-horizontal edges are missed. Fig. 5(d) gives the edge detection result of the proposed method. Fig. 5(e) and Fig. 5(f) show the edge width estimation results. It is worth noting that the edge width is measured in different units. In CPBD and JNBM, the edge width is counted by pixel as shown in (e), while as shown in (3) the proposed method scales the edge width with the

aid of the standard deviation of a Gaussian filter that blurs the edge. Hence, the accuracy of these two methods are evaluated using Relative Square Error (RSE) as follows:

$$RSE = \frac{\sum_{i=1}^N \left| \frac{w(i)-w_{GT}}{w_{GT}} \right|^2}{N}, \quad (8)$$

where N is the number of the detected edge pixels. $w(i)$ is the edge width of the i^{th} detected edge pixel with i ranging from 1 to N . w_{GT} is the ground truth edge width. For the proposed method, w_{GT} should equal to σ since it originates from the standard deviation of the Gaussian blurring kernel as shown in (3). In CPBD and JNBM, the edge width is defined by the spread of the edges based on the smoothing effect of filtering. Hence, the ground truth width w_{GT} is obtained by counting the numbers of pixels with increasing and decreasing grayscale around the edge of the outmost circle in Fig. 5(a), which is an ideal edge for detecting width as its adjacent edge pixels are far away and thus cannot make much influence.

The RSE in (8) evaluates the difference between the detected edge width and the ground truth. Thus, the smaller the RSE is, the more accurate the detection is. Fig. 5(g) shows the RSE results of edge detection when blurring the image with different Gaussian filters ($\sigma = 1, 2, 3, 4$). Apparently, the RSE results of the proposed method are much smaller than those produced by CPBD and JNBM for all the blurring scales.

3.2. Performance Results for Gaussian-Blurred and JPEG2000-Compressed Images

In this section, experiments are conducted to illustrate the performance of the proposed metric using a set of Gaussian blurred and JPEG2000-compressed images from some popular subjective image quality assessment databases.

3.2.1. LIVE database

The UT Austin LIVE database [32] consists of 29 high-resolution RGB color images and these images are distorted using different distortion types, including Gaussian blur and JPEG2000. After distortion, each image is scored by 20–29 subjects. Then, the standard deviation (std) of the processed score and the Difference Mean Opinion Score (DMOS) are recorded for metric performance testing.

3.2.2. TID2008 database

The TID2008 [33] contains 25 reference images and 1700 distorted images (25 reference images, 17 types of distortions for each reference image, 4 different levels of each type of distortion). To get the subjective evaluation results of the proposed metric, 654 observers from three different countries (Finland, Italy and Ukraine) participated in the subjective tests. On average, each distorted image is judged by more than 200 observers. The std and MOS scores of Gaussian-blurred and JPEG2000 distortion types are recorded.

3.2.3. CSIQ database

The CSIQ image database [34] is a new one which is released by the Oklahoma State University with 30 original images. Four or five different levels of distortion are used in different distortion types. There are 35 observers in this experiment. Similarly, all of the distorted blurry images are used in our experiments.

3.2.4. Results

First, we pick an image (768×512 House) from the LIVE database to test the monotonic decreasing behavior of the proposed metric. Specifically, we increasingly blur an image with different Gaussian kernels and use the proposed metric to evaluate the blur quality. As shown in Fig. 6, the proposed metric performed as expected and the value decreases monotonically as the blurriness increases.

To test how well the proposed metric correlates with the recorded subjective scores of these Gaussian-blurred and JPEG2000-blurred images, five performance evaluation metrics [29] are adopted as follows: 1) Pearson Linear Correlation Coefficient (PCC, indicates prediction accuracy); 2) Spearman Rank-Order Correlation Coefficient (SROCC, indicates prediction monotonicity); 3) Root Mean Squared Error (RMSE); 4) Mean Absolute Error (MAE); 5) Outlier Ratio (OR, indicate prediction consistency). The high PCC and SROCC scores and low RMSE, MAE and OR scores indicate that the metric well matches the subjective evaluation. Tables 1–3 summarize the performance of the proposed metric, and give comparison with existing state-of-the-arts methods LPC [15, 16], Marziliano [20], JNBM [23], and

CPBD [24]. The results in Tables 1-3 were published in [24] and the OR comparison is excluded in Table 2 as the OR values are missed in [24].

Table 1: Evaluation of the proposed EMBM metric for the LIVE database

Distortion	Metrics	PCC	SROCC	RMSE	MAE	OR
Gaussian-blurred	LPC metric	0.9200	0.9497	8.5250	6.9335	0.1724
	Marziliano metric	0.8597	0.8659	11.1106	8.2743	0.2184
	JNBM metric	0.8390	0.8368	11.8365	9.3485	0.2471
	CPBD metric	0.9107	0.9437	8.9857	6.8869	0.1609
	Proposed metric	0.9233	0.9297	6.5676	5.0513	0.0575
JPEG2000	LPC metric	0.4233	0.3880	22.1024	18.4596	0.6167
	Marziliano metric	0.7815	0.7744	15.2196	11.7002	0.4670
	JNBM metric	0.7190	0.7255	16.9546	13.7478	0.5022
	CPBD metric	0.8835	0.8862	11.4288	9.0546	0.3260
	Proposed metric	0.8873	0.8191	9.6839	7.5940	0.1498

Table 2: Evaluation of the proposed EMBM metric for the TID2008 database

Distortion	Metrics	PCC	SROCC	RMSE	MAE
Gaussian-blurred	LPC metric	0.8113	0.803	0.6778	0.5202
	Marziliano metric	0.7090	0.7165	0.8176	0.6466
	JNBM metric	0.7171	0.7045	0.8081	0.6254
	CPBD metric	0.8316	0.8406	0.6438	0.5019
	Proposed metric	0.8629	0.8586	0.5931	0.4705
JPEG2000	LPC metric	0.7952	0.7295	1.1621	0.9356
	Marziliano metric	0.8667	0.8694	0.9561	0.7127
	JNBM metric	0.8798	0.8789	0.9111	0.7213
	CPBD metric	0.9223	0.9250	0.7406	0.5831
	Proposed metric	0.9247	0.9245	0.7431	0.5948

For the Gaussian-blurred images, it can be seen that the proposed metric performed well in terms of accuracy, monotonicity and consistency. In the test of LIVE database (Table 1), PCC of the proposed metric achieves 0.9233 which implies the proposed metric is capable of predicting the subjective quality ratings with low error. The MAE and OR are lowest as 5.0513 and 0.0575, respectively. The OR is sixty percent lower than that of CPBD , which illustrates the better consistency over the range of the test images. As shown in Table 2, the proposed metric exhibits the best performance in terms of all respects in the TID2008 test. For the CSIQ database (Table 3), the performance of the proposed metric is similar to that of CPBD.

For the JPEG2000 images, the proposed metric has a performance that is competitive to that of CPBD in all databases, and is significantly better than those of LPC, Marziliano and JNBM metrics. Specifically, the proposed metric exhibits the best PCC, RMSE, MAE and OR for the LIVE and CSIQ databases. In the test of TID2008, our method still has the highest PCC and the others are close to those of CPBD. All above results indicate that the proposed metric performs well in dealing with images with different blur distortions.

Moreover, the proposed metric has lower computational complexity. As shown in Fig. 7, the Matlab implementations¹ of LPC, CPBD and JNBM normally take 4 to 6 seconds to evaluate a 512×512 image on a PC with an Intel Core 2 Duo 2.50-GHz CPU. The proposed method is more efficient and only takes about 2 seconds with Matlab programming.

¹The Matlab codes of LPC, JNBM and CPBD are downloaded from the authors' website.

Table 3: Evaluation of the proposed EMBM metric for the CSIQ database

Distortion	Metrics	PCC	SROCC	RMSE	MAE	OR
Gaussian-blurred	LPC metric	0.8912	0.8833	0.1300	0.1011	0.3067
	JNBM metric	0.8193	0.7720	0.1643	0.1290	0.3867
	CPBD metric	0.8557	0.8645	0.1483	0.1185	0.3800
	Proposed metric	0.8478	0.8494	0.1519	0.1232	0.3600
JPEG2000	LPC metric	0.7155	0.5197	0.2207	0.1830	0.6533
	JNBM metric	0.7710	0.7342	0.2012	0.1575	0.6000
	CPBD metric	0.8585	0.8428	0.1621	0.1216	0.5400
	Proposed metric	0.8760	0.8377	0.1524	0.1207	0.5333

4. Conclusions

In this paper, we addressed the image blur assessment problem by integrating the concept of edge modeling into JNB. A parametric edge model is introduced to overcome the limitations of conventional blur metrics, and the width and contrast for each edge pixel can be computed simultaneously. Unlike previous work, the proposed method does not need to perform block by block, and relies on the salient edges to measure image quality. Various images with different blur distortions were tested to demonstrate the effectiveness of the proposed metric. Experiments on different subjective databases showed that the proposed metric performs well in evaluating different distorted images. In the future, it is worthy to investigate the application of the proposed algorithm in video quality assessment tasks.

Acknowledgment

We thank the editor and all anonymous reviewers for their constructive comments. This work was supported by the NSFC Grant No. 61203253 and 61233014, Research Found of Outstanding Young Scientist Award of Shandong Province (BS2013DX023), Independent Innovation Foundation of Shandong University (IIFSDU) 2013TB004, and Program of Key Lab of ICSP MOE. This work was also in part supported by the Singapore Academic Research Fund under Grant R397000139133 and Grant R397000177133 awarded to Dr. Hongliang Ren.

References

- [1] W. Lin, C. C. Jay Kuo, Perceptual visual quality metrics: A survey, *Journal of Visual Communication and Image Representation* 22(4) (2011) 297–312.
- [2] C. Charrier, O. Lzoray, G. Lebrun, Machine learning to design full-reference image quality assessment algorithm, *Signal Processing: Image Communication* 27(3) (2012) 209–219.
- [3] X. Fei, L. Xiao, Y. Sun, Z. Wei, Perceptual image quality assessment based on structural similarity and visual masking, *Signal Processing: Image Communication* 27(7) (2012) 772–783.
- [4] H. R. Sheikh, M. F. Sabir, A. C. Bovik, A statistical evaluation of recent full reference image quality assessment algorithms, *IEEE Transactions on Image Processing* 15(11) (2006) 3440–3451.
- [5] K. Seshadrinathan, A. C. Bovik, Unifying analysis of full reference image quality assessment, *Proc. IEEE International Conference on Image Processing* (2008) 1200–1203.
- [6] X. Gao, W. Lu, D. Tao, X. Li, Image quality assessment based on multiscale geometric analysis, *IEEE Transactions on Image Processing* 18(7) (2009) 1409–1423.
- [7] L. Ma, S. Li, F. Zhang, K. N. Ngan, Reduced-reference image quality assessment using reorganized DCT-based image representation, *IEEE Transaction on Multimedia*, 13(4) (2011) 824–829.
- [8] L. Ma, S. Li, K. N. Ngan, Reduced-reference image quality assessment in reorganized DCT domain, *Signal Processing: Image Communication* 28(8) (2013) 884–902.
- [9] A. Tanchenko, Visual-PSNR measure of image quality, *Journal of Visual Communication and Image Representation* 25(5) (2014) 874–878.
- [10] P. Le Callet, C. V. Gaudin, D. Barba, Continuous quality assessment of MPEG2 video with reduced reference, *Proc. International Workshop on Video Processing and Quality Metrics for Consumer Electronics* (2005).
- [11] S. Yang, Reduced reference MPEG-2 picture quality measure based on ratio of DCT coefficients, *Electronics Letters* 47(6) (2011) 382–383.
- [12] M. Carnec, P. Le Callet, D. Barba, Visual features for image quality assessment with reduced reference, *Proc. IEEE International Conference on Image Processing* (2005) 421–424.

- [13] R. Soundararajan, A. C. Bovik, RRED indices: reduced reference entropic differencing framework for image quality assessment, Proc. International Conference on Acoustics, Speech, and Signal Processing (2011).
- [14] W. Zhou, G. Jiang, M. Yu, F. Shao, Z. Peng, Reduced-reference stereoscopic image quality assessment based on view and disparity zero-watermarks, Signal Processing: Image Communication 29(1) (2014) 167-176.
- [15] R. Hassen, Z. Wang, M. Salama, No-reference image sharpness assessment based on local phase coherence measurement, Proc. International Conference on Acoustics, Speech, and Signal Processing (2010) 2434-2437.
- [16] R. Hassen, Z. Wang, M. Salama, Image sharpness assessment based on local phase coherence, IEEE Transactions on Image Processing 22(7) (2013) 2798-2810.
- [17] P. V. Vu, D. M. Chandler, A fast wavelet-based algorithm for global and local image sharpness estimation, IEEE Signal Processing Letters 19(7) (2012) 423-426.
- [18] G. Blanchet, L. Moisan, B. Rouge, Measuring the global phase coherence of an image, Proc. IEEE International Conference on Image Processing (2008) 1176-1179.
- [19] G. Blanchet, L. Moisan, An explicit sharpness index related to global phase coherence, Proc. International Conference on Acoustics, Speech, and Signal Processing (2012) 1065-1068.
- [20] P. Marziliano, F. Dufaux, S. Winkler, T. Ebrahimi, Perceptual blur and ringing metrics: application to JPEG2000, Signal Processing: Image Communication 91(2) (2004) 163-172.
- [21] H. Tang, N. Joshi, A. Kapoor, Learning a blind measure of perceptual image quality, Proc. IEEE International Conference on Computer Vision and Pattern Recognition (2011) 305-312.
- [22] A. Mittal, R. Soundararajan, G. S. Muralidhar, A. C. Bovik, J. Ghosh, Blind image quality assessment without training on human opinion scores, Proc. SPIE 8651, Human Vision and Electronic Imaging (2013) XVIII 86510T.
- [23] R. Ferzli, L. J. Karam, A no-reference objective image sharpness metric based on the notion of just noticeable blur (JNB), IEEE Transactions on Image Processing 18(4) (2009) 717-728.
- [24] N. D. Narvekar, L. J. Karam, A no-reference image blur metric based on the cumulative probability of blur detection (CPBD), IEEE Transactions on Image Processing 20(9) (2011) 2678-2683.
- [25] M. A. Saad, A. C. Bovik, C. Charrier, Blind image quality assessment: A natural scene statistics approach in the DCT domain, IEEE Transactions on Image Processing 21(8) (2012) 3339-3352.
- [26] L. He, D. Tao, X. Li, X. Gao, Sparse representation for blind image quality assessment, Proc. IEEE International Conference on Computer Vision and Pattern Recognition (2012) 1146-1153.
- [27] P. Ye, J. Kumar, L. Kang, D. Doermann, Unsupervised feature learning framework for no-reference image quality assessment, Proc. IEEE International Conference on Computer Vision and Pattern Recognition (2012) 1098-1105.
- [28] X. Gao, F. Gao, D. Tao, X. Li, Universal blind image quality assessment metrics via natural scene statistics and multiple kernel learning, IEEE Transactions on Neural Networks and Learning Systems 24(12) (2013) 2013-2026.
- [29] VQEG, "Final report from the video quality experts group on the validation of objective models of video quality assessment," Mar. 2000 [Online]. Available: <http://www.vqeg.org/>
- [30] P. J. L. van Beek, Edge-based image representation and coding, Ph.D. dissertation, Delft Univ. Technol., Delft, The Netherlands (1995).
- [31] W. Zhang, W. K. Cham, Single image refocusing and defocusing, IEEE Transactions on Image Processing 21(2) (2012) 873-882.
- [32] H. R. Sheikh, A. C. Bovik, L. Cormack, Z. Wang, LIVE image quality assessment database, (2003) [Online]. Available: <http://live.ece.utexas.edu/research/quality>
- [33] N. Ponomarenko, V. Lukin, A. Zelensky, K. Egiazarian, M. Carli, F. Battisti, TID2008 - A database for evaluation of full-reference visual quality assessment metrics, Advances of Modern Radioelectronics 10 (2009) 30-45.
- [34] E. C. Larson, D. M. Chandler, Most apparent distortion: full-reference image quality assessment and the role of strategy, Journal of Electronic Imaging 19(1) (2010).

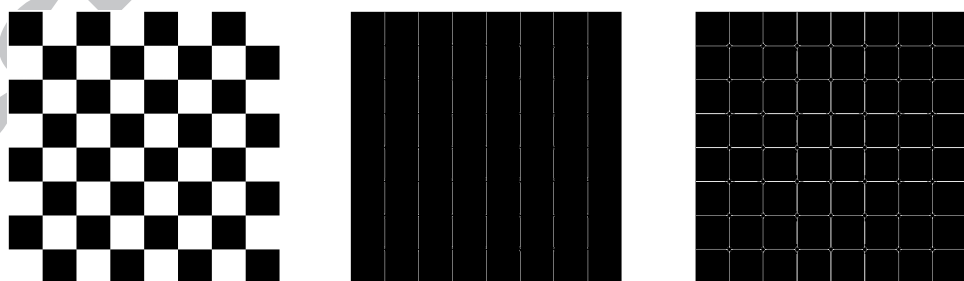


Figure 1: Edge detection on horizontal and vertical lines. Left: Test image; Middle: Result of JNBM and CPBD; Right: Our result.

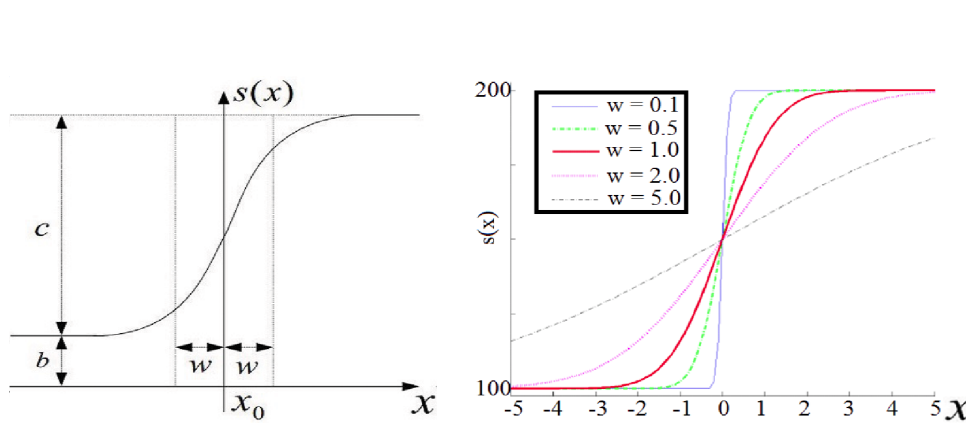
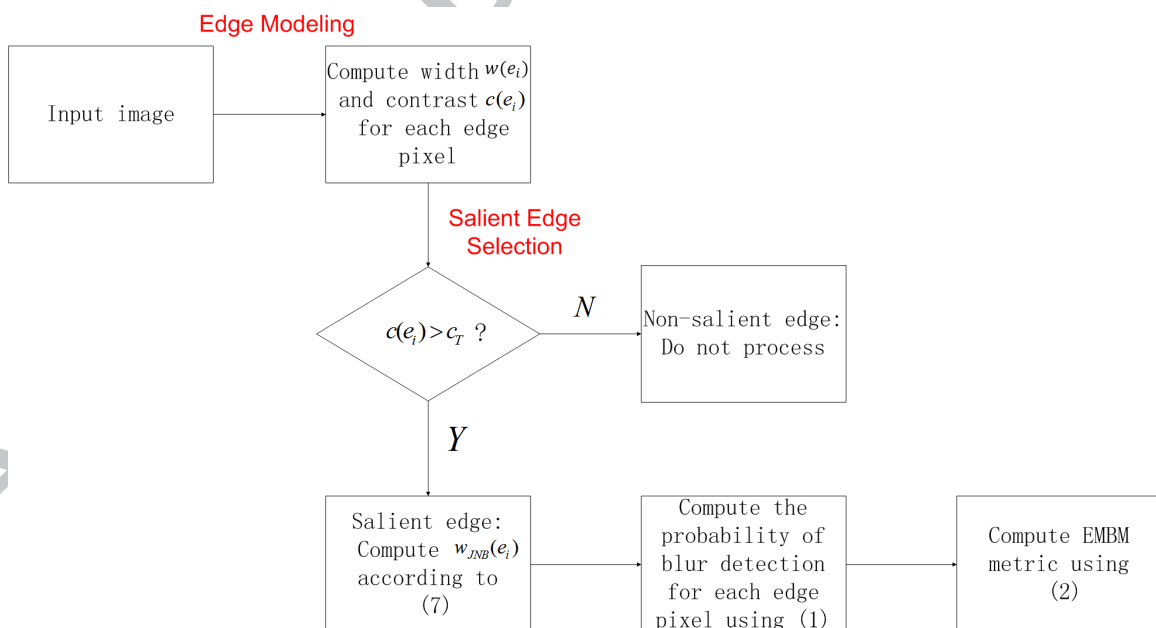
Figure 2: (a) 1-D parametrical edge model; (b) Effect of decreasing w .

Figure 3: Block diagram of the proposed EMBM metric.



Figure 4: Comparison on edge detection. Left: Test image; Middle: Result of JNBM and CPBD; Right: Our result.

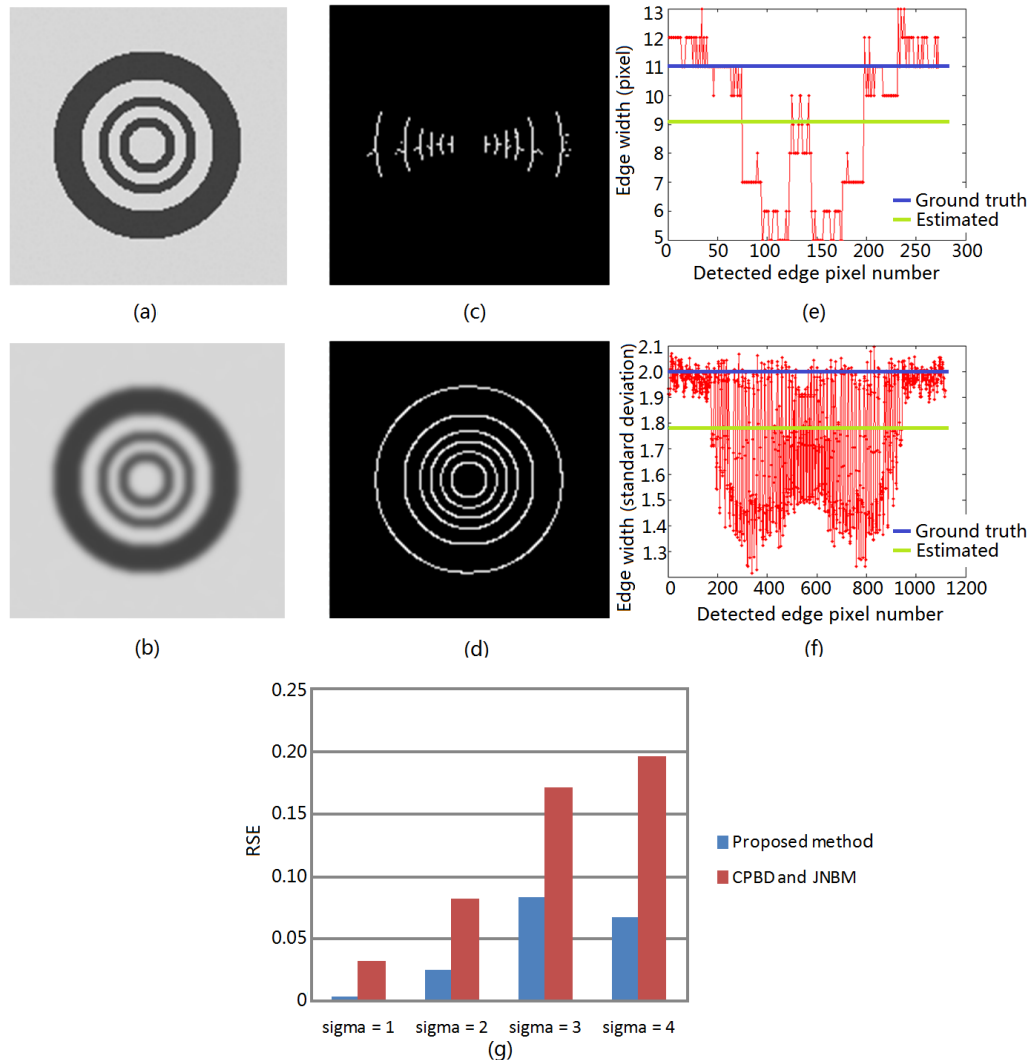


Figure 5: (a) Original image (150×150). (b) Gaussian-blurred image with $\sigma = 2$. (c) Edge detection result of CPBD and JNBM. (d) Edge detection result of the proposed method. (e) Estimated edge width of CPBD and JNBM. (f) Estimated edge width of the proposed method. The blue and green lines denote the ground truth and the average estimation respectively. (g) Comparison of the Relative Square Error (RSE) in different Gaussian-blurred images.

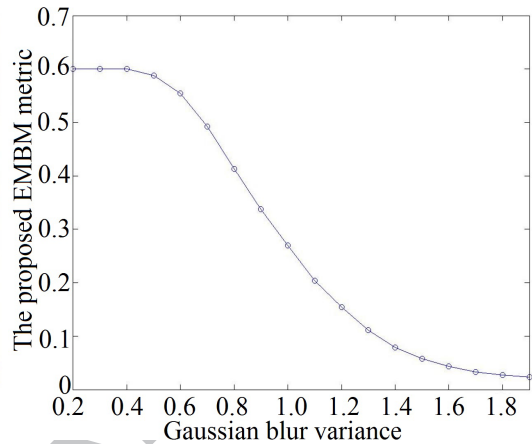


Figure 6: The monotonic decreasing behavior of the proposed metric for increasingly blurred image. Original image (768×512 House image from LIVE) and t The monotonic decreasing behavior of the proposed EMBM metric for increasingly blurry images.



Metric	Time(s)
LPC metric	4.4148
CPBD metric	4.1028
JNBM metric	5.5536
Proposed metric	2.2885

Figure 7: (a) Test image. (b) Running time.

Highlights

- We propose a no-reference blur metric by integrating edge modeling into JNB.
- A parametric edge model is introduced for edge description and computation.
- We advocate using the salient edge pixels to simulate the blur assessment of HVS.
- With the pixel-adaptive width and contrast, the metric is simple yet accurate.